JOURNAL OF AGRICULTURAL AND FOOD CHEMISTRY

J. Agric. Food Chem. **2006,** *54,* 8589−8597 **8589**

Influence of Aging and Salting on Protein Secondary Structures and Water Distribution in Uncooked and Cooked Pork. A Combined FT-IR Microspectroscopy and ^{1}H NMR Relaxometry Study

ZHIYUN WU,*,† HANNE CHRISTINE BERTRAM,† ACHIM KOHLER,‡ ULRIKE BÖCKER,‡ RAGNI OFSTAD,‡ AND HENRIK J. ANDERSEN§

Department of Food Science, Research Center Foulum, Danish Institute of Agricultural Sciences, P.O. Box 50, DK-8830 Tjele, Denmark, Centre for Biospectroscopy and Data Modelling, Matforsk AS, Norwegian Food Research Institute, Osloveien 1, NO-1430 Ås, Norway, and Arla Foods amba, Skanderborgvej 277, DK-8260 Viby J, Denmark

Fourier transform infrared (FT-IR) microspectroscopy and low-field (LF) proton NMR transverse relaxation measurements were used to study the changes in protein secondary structure and water distribution as a consequence of aging (1 day and 14 days) followed by salting (3%, 6%, and 9% NaCl) and cooking (65 °C). An enhanced water uptake and increased proton NMR relaxation times after salting were observed in aged meat (14 days) compared with nonaged meat (1 day). FT-IR bands revealed that salting induced an increase in native β-sheet structure while aging triggered an increase in native α-helical structure before cooking, which could explain the effects of aging and salting on water distribution and water uptake. Moreover, the decrease in T_2 relaxation times and loss of water upon cooking were attributed to an increase in aggregated β-sheet structures and a simultaneous decrease in native protein structures. Finally, aging increased the cooking loss and subsequently decreased the final yield, which corresponded to a further decrease in T_2 relaxation times in aged meat upon cooking. However, salting weakened the effect of aging on the final yield, which is consistent with the increased T_2 relaxation times upon salting for aged meat after cooking and the weaker effect of aging on protein secondary structural changes for samples treated with high salt concentration. The present study reveals that changes in water distribution during aging, salting, and cooking are not only due to the accepted causal connection, i.e., proteolytic degradation of myofibrillar structures, change in electrostatic repulsion, and dissolution and denaturation of proteins, but also dynamic changes in specific protein secondary structures.

KEYWORDS: FT-IR microspectroscopy; NMR T_2 relaxation; protein secondary structure; cooking; aging; salting; meat.

INTRODUCTION

Optimization of meat processing aiming to improve quality and yield is very important for the meat processing industry, thus fulfilling the demands of the consumers and receiving a profitable earning, respectively. Aging of meat weakens the myofibrillar structure, and it is well-known that aging improves the tenderness and texture of meat (*1*, *2*). In addition, a number of studies have reported an improvement in water-holding capacity (WHC) upon aging (*3*−*9*). This improvement in WHC has been suggested to be a result of proteolytic degradation of cytoskeletal proteins, which subsequently enables swelling of the myofibrils and thereby allows the meat structure to retain more myowater (*1*, *10*−*12*). Moreover, it has recently been reported that prolonged aging is associated with an increased cooking loss (*6*). However, besides the effect on WHC of fresh meat, the impacts of an aging period prior to processing of meat have not been studied extensively (*13*).

Fourier transform infrared (FT-IR) microspectroscopy has become an important analytical technique for studying the chemical composition of foods (*14*−*20*) and more recently in the study of protein secondary structures of human and animal tissue (*21*−*23*). Structural and compositional changes of mammalian protein structures can be determined from the frequency and intensity analysis of absorption bands depending on the protein backbone conformation and hydrogen-bonding pattern. Recently, FT-IR has been used to characterize the heat-induced denaturation of myofibrillar and connective tissue proteins of

* To whom correspondence should be addressed. Phone: (45) 89 99 1142. Fax: (45) 89 99 1564. E-mail: Zhiyun.Wu@agrsci.dk.
† Danish Institute of Agricultural Sciences.
‡ Norwegian Food Research Institute.
§ Arla Foods amba.

10.1021/jf061576w CCC: $33.50
Published on Web 10/10/2006

Table 1. Meat Processes of Aging, Salting, and Heating and the Corresponding Symbols as Well as the Names and Numbers of Samples

aging	salting (%)	heating (°C)
1 day (A) $n = 40$	0 (A0) $n = 10$	25 (A025) $n = 5$
		65 (A065) $n = 5$
	3 (A3) $n = 10$	25 (A325) $n = 5$
		65 (A365) $n = 5$
	6 (A6) $n = 10$	25 (A625) $n = 5$
		65 (A665) $n = 5$
	9 (A9) $n = 10$	25 (A925) $n = 5$
		65 (A965) $n = 5$
14 days (B) $n = 40$	0 (B0) $n = 10$	25 (B025) $n = 5$
		65 (B065) $n = 5$
	3 (B3) $n = 10$	25 (B325) $n = 5$
		65 (B365) $n = 5$
	6 (B6) $n = 10$	25 (B625) $n = 5$
		65 (B665) $n = 5$
	9 (B9) $n = 10$	25 (B925) $n = 5$
		65 (B965) $n = 5$

beef (*24*) and salt- and heat-induced changes in myofibrillar protein of pork (*25*, *26*).

Likewise, NMR relaxometry has gained extensive interest in the field of food science within the past 2 decades due to potential of the methods to characterize the distribution and mobility of one of the main food components, water. In meat, the water, also named myowater, is entrapped in the myofibrillar protein network, where its distribution and mobility are highly associated with the structural features of the myofibrillar protein network. Especially, low-field ^{1}H NMR T_2 relaxation has been used to study myowater distribution and the mobility of myowater in meat (for an extensive review see *27*). The altered T_2 distribution in different meat products reflects the different water compartmentalization and water mobility as a result of the chemical exchange with the protein structures of the different products (*28*, *29*).

The objective of this mechanistic study was to exploit the influence of aging and salting procedure on changes in myofibrillar protein structures and myowater distribution in green (uncooked) and cooked pork using FT-IR microspectroscopy and low-field ^{1}H NMR T_2 relaxometry, respectively, and discuss this in relation to technological meat quality.

MATERIALS AND METHODS

Meat Sampling. The right and left *M. longissimus dorsi* (LD) from a pig, which is an offspring of a Duroc/Landrace boar cross-bred with Landrace/Yorkshire sow, were used in this study. At the time of slaughter, the pig had a live weight of approximately 100 kg. The pig was slaughtered in the experimental abattoir at Research Center Foulum. The pig was stunned by 80% CO_2 for 3 min, exsanguinated, and scalded at 62 °C for 3 min. Cleaning and evisceration of the carcass were completed within 30 min postmortem. The carcass was split and kept at 12 °C. Within 3 h postmortem the carcass was transferred to a chill room, where it was stored at 4 °C.

At 24 h postmortem, the pH measured in the two LDs was found to be 5.62 and 5.61, respectively. Drip loss of the two muscles was 6.2% and 6.7%, respectively, measured according to the method described by Honikel (*30*). The right and left *M. longissimus* were used for nonaged (1 day) and aged (14 days) meat, respectively. The left *M. longissimus* was placed in a plastic bag and stored at 4 °C for 14 days; minor exuded water was observed after 14 days. The right *M. longissimus* was cut into 5 parallel chops of 10 cm. Subsequently, eight samples with a size of approximately 1 × 1 × 4 cm were cut from each chop and weighed out (weight 1), resulting in a total of 40 samples. Five replicates from the 5 different chops were finally assigned to the same experimental conditions; see Table 1. Thirty of the nonaged samples were cured using different sodium chloride concentrations. The remaining 10 samples were used as control samples without salt treatment. The same procedure was applied on aged meat, resulting in 40 additional samples. The resultant 16 experimental conditions on 80 samples and the corresponding symbols as well as the names and numbers of samples are listed in Table 1.

Processing of Meat Samples. Three salting brines with 3%, 6%, and 9% sodium chloride, respectively, were made in 10 mM sodium acetate and added 0.05% NaN_3, as preservative agent, and the pH was adjusted to 5.5 in all salting brines. All 60 samples were placed individually in a container labeled with the corresponding sample name and salted in 40 mL of brine. The containers were placed on a vibrating table at 4 °C. After 48 h, the samples were removed from the brine, dabbed, and weighed out (weight 2). The salting-induced weight gain was calculated as the percentage weight gain according to the following equation:

$$\text{weight gain (\%)} = \frac{\text{weight2} - \text{weight1}}{\text{weight1}} \times 100$$

Subsequently, each sample was placed in a small glass tube closed by a screw cap, and half the samples were heated in a water bath at 65 °C for 20 min, followed by a temperature equilibrium at 25 °C in another water bath for 20 min, while the remaining samples were only brought into a water bath at 25 °C for 20 min with the purpose of temperature equilibrium. Finally, the cooked samples were weighed again (weight 3) after discarding the water lost during cooking. Cooking loss and yield were calculated by the equation

$$\text{cooking loss (\%)} = \frac{\text{weight2} - \text{weight3}}{\text{weight2}} \times 100$$

$$\text{yield (\%)} = \frac{\text{weight3}}{\text{weight1}} \times 100$$

^{1}H NMR T_2 Relaxation Measurements. The ^{1}H NMR T_2 relaxation measurements were performed at 25 °C on a Maran Benchtop Pulsed NMR Analyzer (Resonance Instruments, Witney, UK) with a resonance frequency for protons of 23.2 MHz. The NMR instrument was equipped with an 18 mm variable temperature probe. Transverse relaxation (T_2) was measured using the Carr-Purcell-Meiboom-Gill sequence (CPMG). The T_2 measurements were performed with a τ-value (time between 90° pulse and 180° pulse) of 150 s and using a repetition delay of 3 s. The data were acquired as the amplitude of every second echo (to avoid influence of imperfect pulse settings) in a train of 4096 echoes as an average of 16 repetitions. After NMR relaxation measurements, the samples were subdivided into small samples and preserved at −80 °C in liquid nitrogen for FT-IR spectroscopy measurements.

The obtained NMR transverse relaxation decays were analyzed by distributed exponential fitting analysis, which was performed according to the regularization algorithm of Butler, Reeds, and Dawson (1981) and implemented in the RI Win-DXP software program (release version 1.2.3) from Resonance Instruments Ltd., UK. This analysis yields a plot of the relaxation amplitude for individual relaxation processes versus relaxation time.

FT-IR Measurements. FT-IR measurements were performed with an IR microscope II (Bruker Optics, Germany), coupled to an Equinox 55 spectrometer (Bruker Optics, Germany). The microscope was equipped with a computer-controlled *x*,*y* stage. The Bruker system was controlled with an IBM compatible PC running OPUS-NT software. Tissue cryosections of 10 μm thickness were thaw-mounted on CaF_2 substrates. The samples were dried in a desiccator using anhydrous silica gel in the desiccator to avoid water absorption in IR. To reduce water vapor, which absorbs in the IR band and hereby interferes with some of the protein bands, the sample compartment was continuously purged with dry air. The spectra were recorded from single fibers in the region between 4000 and 600 cm^{-1} with a spectral resolution of 6 cm^{-1} using a mercury-cadmium-tellurium detector and an aperture of 5.0 mm. For each spectrum 256 scans were accumulated and averaged. Three NMR subsamples from each experimental condition were used for FT-IR spectra measurements, and three spectra were collected from each subsample, resulting in a total of 144 spectra for all 16

experimental conditions. The original IR spectra were preprocessed by extended multiplicative signal correction (EMSC) using The Unscrambler version 9.2 (CAMO Software AS, Norway) to avoid the physical light scattering effects. After EMSC the second derivative of the spectra was taken in order to resolve the overlapping of bands. After preprocessing, the spectra from the same experimental conditions were averaged.

Data Analysis. To analyze the main variation in the data sets and the correlation between the design variables aging, salting, cooking, and FT-IR absorbance bands and ^{1}H NMR T_2 relaxation times, the data analysis was performed using principal component analysis (PCA) and partial least-squares regression (PLSR2) of The Unscrambler version 9.2. In PLSR2 the response variables **Y** are expressed as a linear function of the **X** variables (*25*). The so-called correlation loading plots are used to find the correlation between **X** and **Y** variables to the corresponding PLS components. To investigate the correlation between design indicator variables and FT-IR and NMR variables, the design and FT-IR were used as **X**, and NMR T_2 variables were used as **Y**. The design variables were weighted by their standard deviations prior to PLSR2.

Traditional statistical analyses of the data were carried out with the SAS software version 8.2 (SAS Institute Inc., Cary, NC). The statistical model used was the PROC GLM procedure. The statistical models for salt-induced weight gain and cooking loss included the fixed effects of brine concentration (0%, 3%, 6%, and 9%) and aging time (1 day and 14 days). The statistical models for specific IR bands included the fixed effects of heat (25 and 65 °C), brine concentration (0%, 3%, 6%, and 9%) and aging time (1 day and 14 days). Two-way and three-way interactions were included when significant. In addition, the linear correlations between weight gain and the mean T_2 relaxation time constants were tested using the PROC REG procedure.

RESULTS

Weight Gain and Cooking Loss. The weight gain, cooking loss, and total yield of the nonaged and aged samples as a function of salt concentration are presented in Figure 1. The 14-day-aged samples showed a significantly higher salt-induced weight gain and higher cooking loss compared with the nonaged samples. A significant effect of salt concentration on weight gain and cooking loss was also observed. The 6% salt concentration resulted in slightly higher weight gain and slightly lower cooking loss for both nonaged and aged samples compared with the other salt concentrations investigated. The cooking loss of the salted samples was significantly higher compared with the unsalted (0%) samples. Minor differences in cooking loss were observed between the different salt concentrations (3%, 6%, and 9%). In general, the total yield was lower for the aged samples compared with the nonaged samples. However, the difference in yield between the two aging periods was most pronounced in meat samples without salting (0%) and decreased in salted samples.

^{1}H NMR T_2 Distribution. The distributed proton T_2 relaxation times of green and cooked samples are shown in Figures 2A and 2B, respectively. Figure 2A shows that noncured samples are characterized by three distinct populations centered at 1.5−2.5 ms (T_{2B1}), 40−60 ms (T_{21}), and 200−300 ms (T_{22}) and that the length of aging did not have any pronounced effect on the T_2 characteristics. In contrast, the length of aging influenced the water characteristics in the cured samples, as aged samples were characterized by a slight shift in the T_{21} population toward longer relaxation times compared with nonaged samples. The effects of salting on T_2 characteristics were evident by a slight decrease in T_{2B1} (1−2 ms), a pronounced increase in T_{21} (70−120 ms) and T_{22} (500−1000 ms), and the appearance of an additional population centered at 8−10 ms (T_{2B2}) compared with noncured samples. To investigate the interaction between length of aging and salting procedure, the mean T_{21} relaxation

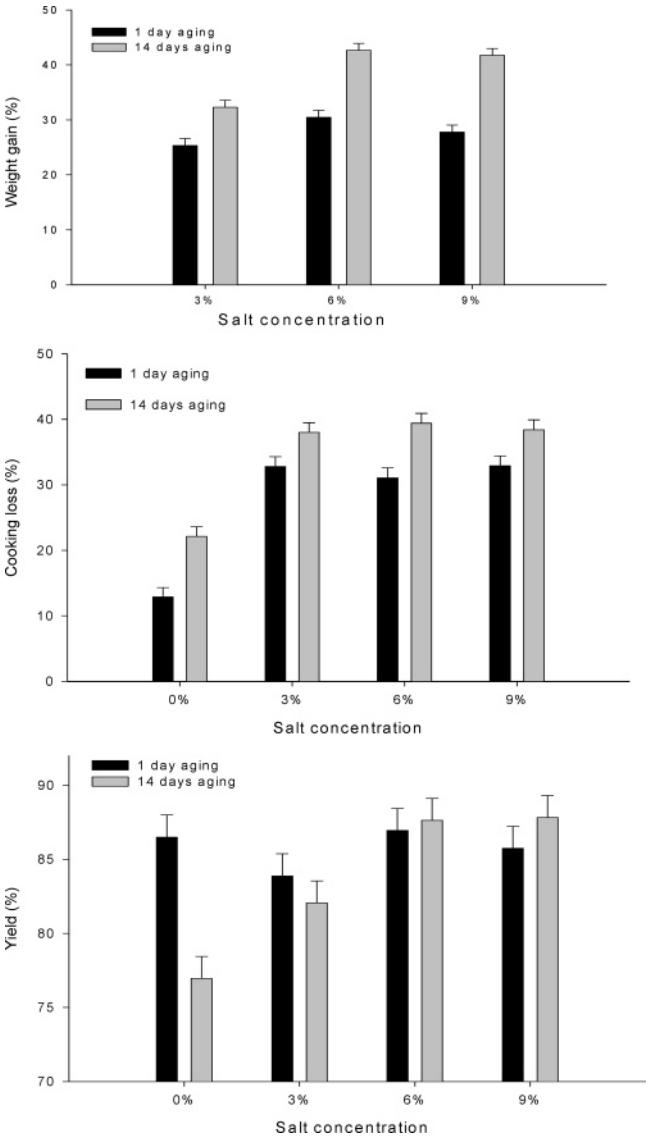

Figure 1. Weight gain (%), cooking loss (%), and yield (%) as a function of salt concentration for both aged samples. LS mean values are given. Bars show standard errors.

times were calculated in the green samples for both aged and nonaged samples and presented as a function of salting-induced weight gain (Figure 3). For all salt concentrations a significantly higher mean T_{21} relaxation time and higher salting-induced weight gain were obtained in aged samples compared with nonaged samples. Independent of aging time, the highest mean T_{21} relaxation time and the highest salting-induced weight gain were obtained at a salt concentration of 6%. Cooking resulted in a more heterogeneous T_{21} distribution, as seen by a significant broadening of the signal compared with green samples (Figure 2B). The nonaged and noncured samples (A065) and samples cured with 9% NaCl (A965) showed a rather broad T_{21} distribution with two shoulders centered at 20−40 and 60−80 ms. However, independent of salting procedure, no splitting of T_{21} distribution was observed in aged samples, even though a slight tendency to a more heterogeneous T_{21} relaxation was evident upon aging for all cured samples.

FT-IR Microspectroscopy. Figure 4 presents the second derivative of the FT-IR spectra of green samples (Figure 4A) and cooked samples (Figure 4B) in the amide I region (1700−1600 cm^{-1}). The minima in the second derivatives refer to maxima in the original spectra. Figure 4 shows representative

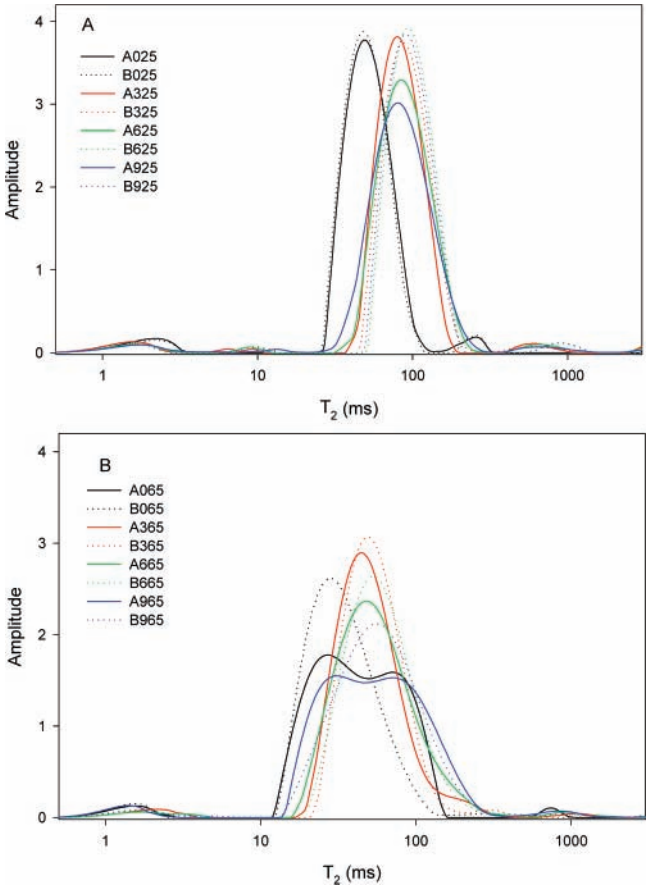

Figure 2. Distributed T_2 relaxation times of samples (A) without heat treatment and (B) after heat treatment at 65 °C. Each curve represents the average of five measurements.

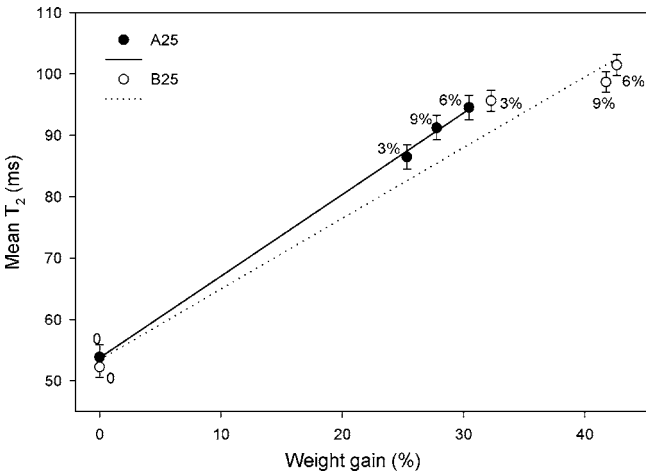

Figure 3. Mean T_2 relaxation times as a function of weight gain for uncooked samples.

IR spectra, which reveal that nine bands at the frequencies of 1695, 1682, 1668, 1660, 1653, 1639, 1628, 1619, and 1610 cm^{-1} changed according to the tested parameters. Significant changes in intensity of the absorption band around 1653 cm^{-1} arising from α-helical structures caused by aging, salting, and heating were observed. Aging increased the intensity, whereas both salting and heating reduced the intensity of the band at 1653 cm^{-1}. In addition, salting tended to change the absorption frequency of the band around 1653 cm^{-1}, as the frequency of this band shifted from 1651 cm^{-1} in unsalted samples to 1654 cm^{-1} in 9% cured samples (Figure 4A). This observation was less pronounced in cooked samples (Figure 4B). Moreover, a

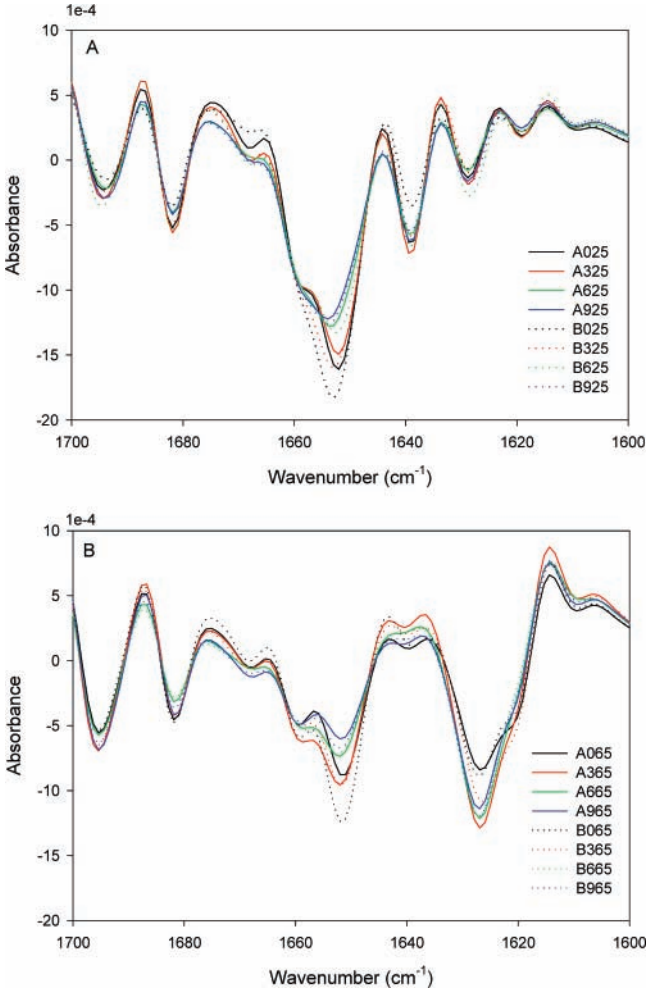

Figure 4. Second derivative of the FT-IR spectra in the amide I region (1700–1600 cm^{-1}) of samples (A) without heat treatment and (B) after heat treatment at 65 °C. Prior to taking the second derivative, the spectra were preprocessed by EMSC. Each spectrum represents the average of nine spectra.

visible inspection showed that the bands at 1639 cm^{-1} and 1628 cm^{-1} were also clearly affected by heating.

Figure 5 presents the score plots of PCA applied on the 72 spectra of green samples (Figure 5A) and 72 spectra of cooked samples (Figure 5B) using the amide I region as variables. In Figures 5A and 5B, a clear clustering according to aging was observed for unsalted samples and for samples treated with 3% salt concentration. Furthermore, the clustering according to salt concentration was distinct only for low salt concentration under both aging conditions. No clear clustering according to salting procedure and aging was observed.

To elucidate the effects of aging, salting, and cooking on all nine selected IR bands further, the effects of these factors were investigated using PROC GLM. Table 2 summarizes the assignments of the nine protein absorption bands in the amide I region and the significant levels for the effects of cooking, salting, and aging on these nine bands. All nine bands were significantly affected by cooking, the intensities of bands at 1619, 1628, 1668, and 1694 cm^{-1} increased, and the bands at 1610, 1639, 1653, 1659, and 1682 cm^{-1} decreased with heating temperature. Seven bands were significantly affected by salting, the bands at 1628, 1668, and 1694 cm^{-1} increased, and bands at 1653, 1610, and 1619 cm^{-1} decreased with increasing salt concentration. For the band at 1639 cm^{-1} strong two- and three-way interactions between cooking, salting, and aging were

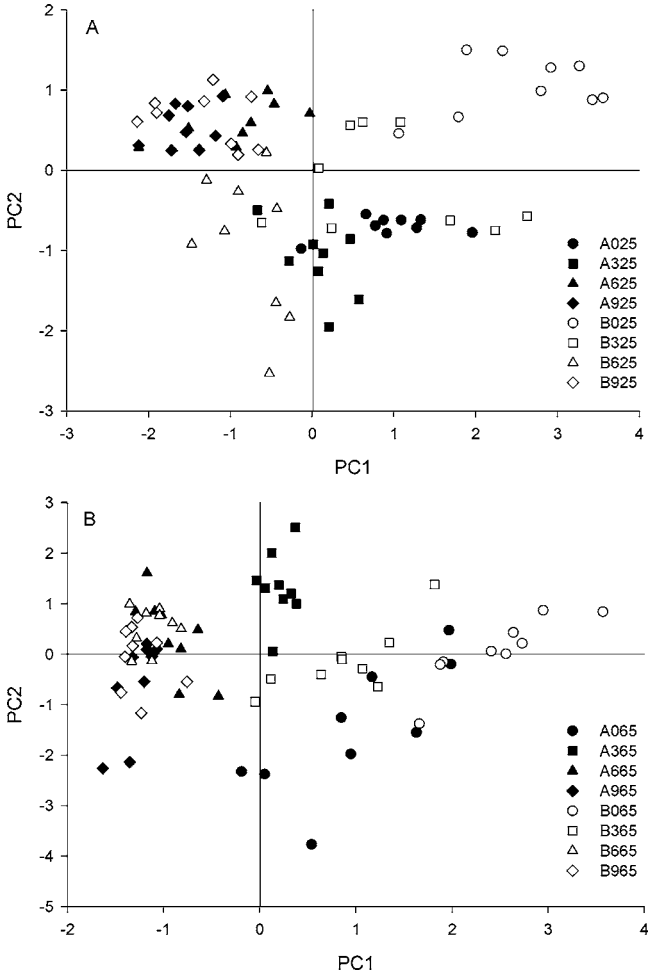

Figure 5. PCA score plots using spectra in amide I region as variables for samples (A) without heat treatment and (B) after heat treatment. For uncooked samples the explained variance by PC1 and PC2 is 56% and 21%, respectively; for cooked samples the explained variance by PC1 and PC2 is 48% and 31%, respectively.

found. The intensity of the band at 1639 and 1682 cm^{-1} increased with salt concentration in uncooked meat samples and decreased in cooked meat. In green samples the bands at 1653, 1639, and 1610 cm^{-1} were significantly affected by aging, while for cooked samples the bands at 1653, 1668, and 1694 cm^{-1} were significantly affected by aging. Figure 6 presents the absorbance of these six bands mostly affected by aging as a function of salting procedure. Increases in the absorbance of α-helical structures around 1653 cm^{-1} and decreases in the absorbance of bands at 1639 and 1610 cm^{-1} caused by aging were observed in green samples (Figure 6A). In heat-treated samples, the effect of aging was less evident. The increased intensity of α-helical structure around 1653 cm^{-1} for aged meat became less pronounced upon salting, while the decreased intensity of the band at 1668 cm^{-1} was reduced upon salting. Moreover, the increase of the absorption at 1694 cm^{-1} was not pronounced during aging (Figure 6B).

Correlation between NMR and FT-IR Data. To investigate the potential correlation between changes in protein secondary structures and water distribution in the pork samples, PLSR2 was carried out individually for uncooked and cooked samples because cooking dominates the main variation. Figures 7A and 7B show the correlation loading plots (first and second PLS component) of PLSR2 with the selected nine FT-IR bands of the amide I region and the design parameters (salt concentration and aging) as **X** and the distributed NMR T_2 relaxation times as **Y** for green and cooked samples, respectively. For green samples, the validated explained variances are 46%/27% for **X** and 63%/12% for **Y** by the first and the second component, respectively. The strong absorption band of α-helices at 1653 cm^{-1} was closely related to the relaxation times of T_{21} centered at 26−66 ms and T_{22} centered at 232−285 ms, which were mainly present in green samples. The absorption bands at 1668, 1694, 1628, and 1639 cm^{-1} correlated to the T_2 relaxation times within the ranges of 7−11, 68−183, and 508−973 ms, which were mainly observed in cured samples. Aging tended to affect the water characteristics in the same way as salting, as seen by increased T_2 relaxation times. For the cooked samples, the validated explained variances are 45%/27% for **X** and 32%/25% for **Y** by the first and the second component, respectively. The bands at 1682, 1619, 1610, and 1639 cm^{-1} were related to the T_2 relaxation times within the range of 13−31 ms. The bands at 1653, 1659, and 1628 cm^{-1} were found to correlate with the

Table 2. Significant Levels (*p*-Values) for Heating, Salting, and Aging on the Intensities of Selected Nine FT-IR Bands in the Amide I Region[a]

IR bands in amide I region (cm^{-1})	tentative assignment	heating	salt	aging	heating* salt	heating* aging	salt* aging	heating* salt* aging
1694	aggregated β-sheet	***	***	*	**	*	***	**
1682	antiparallel β-sheet	***	***	NS	***	NS	**	***
1668	loop structures	***	***	**	***	NS	***	**
1659	more stretched α-helices or loop structures	***	NS	NS	NS	NS	NS	NS
1653	native α-helices	***	***	**	NS	NS	*	NS
1639	antiparallel β-sheet	***	***	***	***	***	***	***
1628	aggregated β-sheet	***	***	NS	***	NS	***	**
1619	aggregated β-sheet	***	***	NS	***	NS	NS	*
1610	possibly related to tyrosine	***	***	**	***	*	NS	NS

[a] Symbols of *p*-value: (*) 0.01 < *p* < 0.05; (**) 0.001 < *p* < 0.01; (***) *p* < 0.001. NS = insignificant.

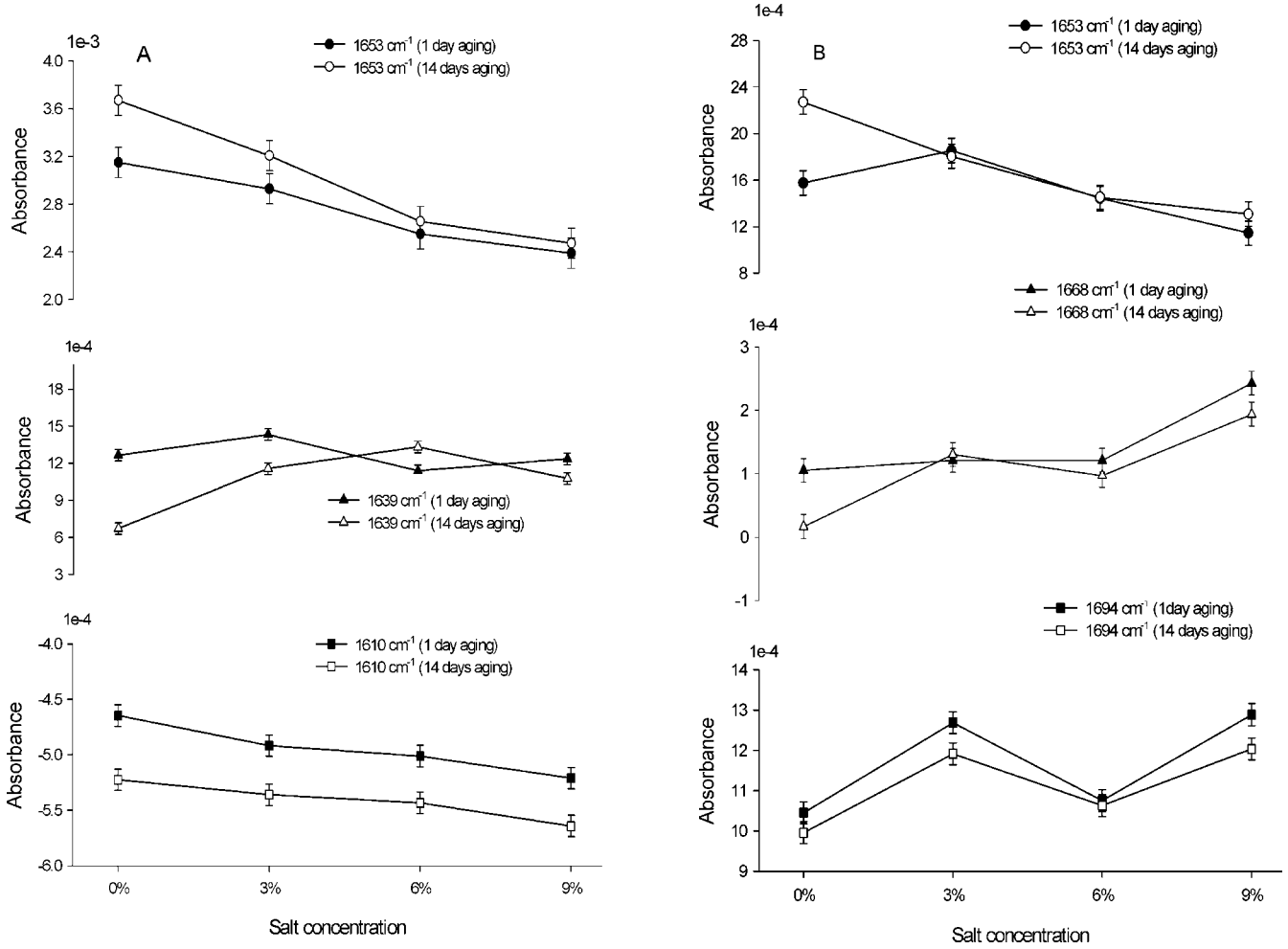

Figure 6. Absorbance of the selected FT-IR bands (negative second derivative) as a function of salt concentration for both aged samples. (A) Significant bands on aging for uncooked samples; (B) significant bands on aging for cooked samples.

T_2 relaxation times of 32−84 ms. The absorption bands at 1668 and 1694 cm^{-1} showed a positive correlation with the T_2 relaxation times within the range of 86−94 ms.

DISCUSSION

The technological quality of meat including the water characteristics is closely associated with the length of the aging period, which together with salting and cooking procedure causes changes within the protein structures of importance for the overall quality of meat products. However, the interactions between length of aging, salting, and cooking procedures have hardly been studied in detail. The present study has for the first time investigated the combined effects of length of aging period and salting on the changes in muscle protein structures and water distribution both in green and cooked pork samples using FT-IR spectroscopy and low-field ^{1}H NMR T_2 relaxometry, respectively. ^{1}H NMR T_2 relaxometry has shown to be able to visualize the changes in water distribution within meat due to the changes in meat structure induced by aging (*6*), salting (*31*), and cooking procedure (*25*, *27*, *32*, *33*). Likewise, FT-IR microspectroscopy has been shown to probe the protein secondary structural changes of meat products using frequency and intensity analysis of the absorption bands in the amide I region of IR spectra (*24*−*26*).

Previous studies have revealed an increase in WHC of fresh meat as a function of aging (*7*−*10*). This is reflected in a redistribution of the myowater, with the intra-myofibrillar water becoming more homogeneous after 14 days of aging (*6*), most probably due to degradation of myofibrillar proteins and cytoskeletal proteins, which naturally will weaken the cytoskeletal restrictions within the muscle protein matrixs (*1*, *10*). The present study clearly shows that aging also influences the protein secondary structures through an increase in α-helices (1653 cm^{-1}) and a decrease in the antiparallel β-structures (1639 cm^{-1}), loop structures (1668 cm^{-1}), and tyrosine exposure (1610 cm^{-1}) (Figure 6A). Combining all these structural observations, it seems that during aging an increase in α-helices involving a decrease in tyrosine exposure, i.e., decrease the exposure of hydrophobic residues to the aqueous environment, together with the weakening of cytoskeletal restrictions, allows a more homogeneous water−protein exchange, as reflected in the more well-defined water distribution progressing throughout aging (*6*).

As mentioned previously, the effect of aging prior to the processing of meat on the subsequent yield has to the authors' knowledge only been studied to a limited extent (*13*). The comparison of nonaged and aged pork revealed a significantly higher salt-induced swelling in the aged pork samples and maximum swelling at salt concentrations of 3% and 6% (Figure 1), which by the NMR measurements could be ascribed to the increased T_{21} relaxation times of water within the myofibrillar network and the high intensities of T_{21} distribution for aged samples (Figure 2). Moreover, the FT-IR measurements revealed that the improved weight gain upon salting of aged pork corresponds to an enhanced formation of aggregated β-structures

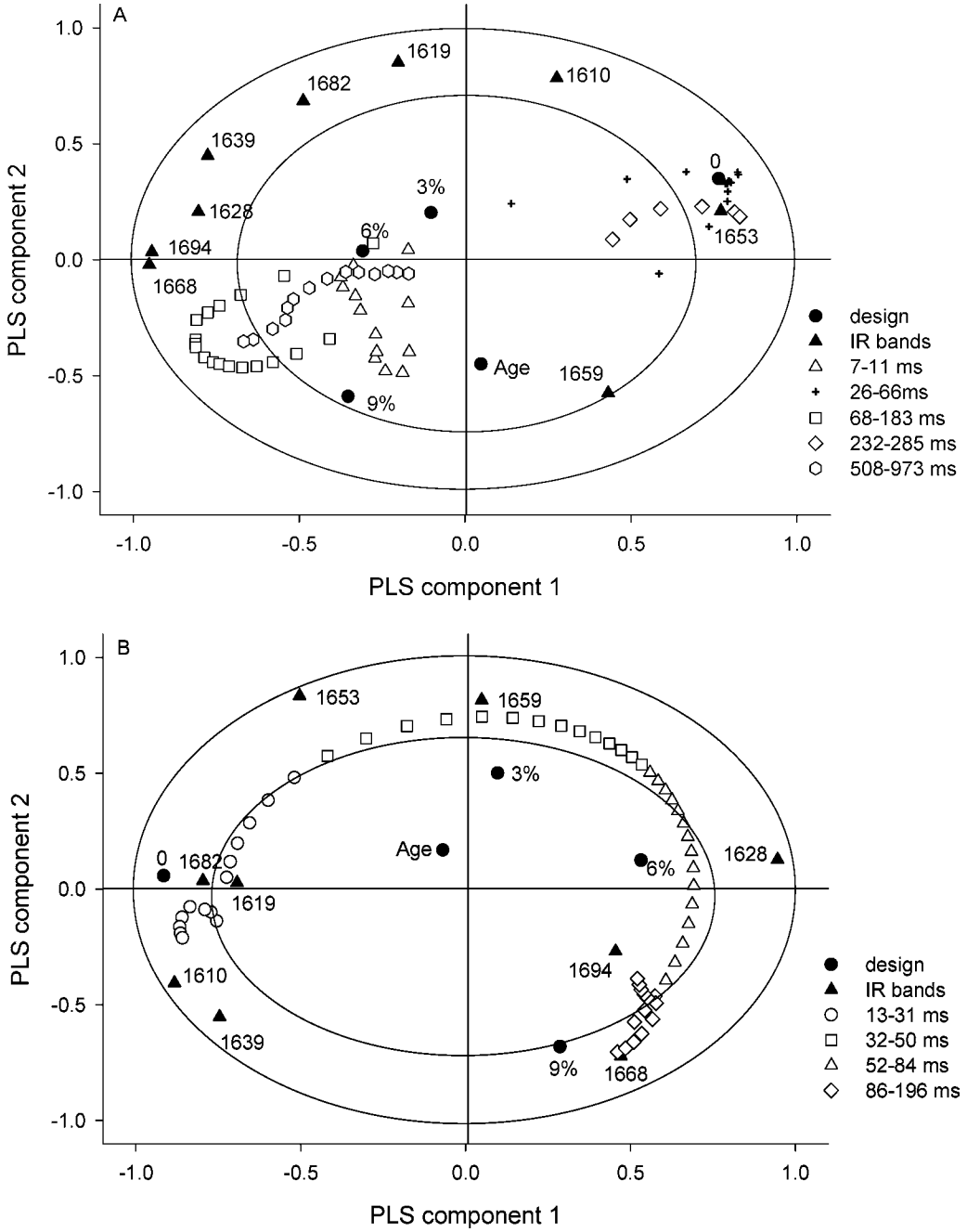

Figure 7. Correlation loading plot (first and second PLS component) of PLSR2 with selected variables of the (negative) second derivative of the amide I region of the FT-IR spectra and design as **X** and distributed NMR T_2 relaxation times as **Y**. (A) For uncooked samples, the validated explained variances are 46%/27% for **X** and 63%/12% for **Y**, the first and the second component, respectively; (B) for cooked samples, the validated explained variances are 45%/27% for **X** and 32%/25% for **Y**, the first and the second component, respectively.

at the expense of α-helices in aged meat (Figure 6A). The observed sodium chloride-induced formation of β-structures at the expense of α-helices with increasing ionic strength has previously been reported for other protein systems (*34*, *35*). Thus, the level of α-helices within the protein matrix seems critical in the salting process, as the transformation of these structures into aggregated β-structures appears to be a driving factor during salting, which allows more water to be trapped in the myofibrillar protein network. Consequently, the present study shows for the first time that besides the well-known effect of sodium chloride on myofibrillar protein repulsion and dissolution on the water characteristics in meat (*32*, *36*−*38*), the specific myofibrillar protein structures are also decisive for the myofibrillar protein network ability to trap water and the characteristics of the intra-myofibrillar water population. In addition, the changes in absorbance frequency of an α-helical structure caused by salt treatment in this study may indicate that α-helices undergo conformational changes, and the strength of the involved hydrogen bonding weakens with increasing salt concentration. To elucidate the effects of aging and salting, a PCA analysis of green samples was performed, which revealed that the effect of aging depends on the salt concentration, as a more pronounced clustering according to aging was observed at lower salt concentrations. This implies that a high salt concentration blurs the effect of aging on changes in protein secondary structures, which might be due to increasing dissolution of the myofibrillar proteins that hereby noticeably eliminate effects on the different protein structures.

Cooking has previously been shown to have dramatic effect on protein structures and water characteristics of meat, resulting

in pronounced loss of water from the intra- and inter-myofibrillar protein network (*25*). Likewise, upon heating we observed in the present study a prominent increase in aggregated β-sheet structures and decrease in α-helixes together with a simultaneous broadening in the T_{21} distribution and decrease in relaxation times, which resemble the physical shrinkage of the intra-myobrillar protein network described by Offer (*36*).

Interestingly, we registered bimodal T_{21} distributions upon cooking of the noncured and 9% of the cured samples, which had not been aged. We assume that this splitting of the T_{21} distribution upon heating can be associated with the interaction of native and aggregated structures or transition states in the ongoing protein denaturation. The observation of no splitting of the T_{21} population in aged meat samples implies that structural constraints may cause this splitting, which is eliminated during aging as a consequence of a weakening of cytoskeletal restrictions. This is further supported by the fact that the bimodal T_{21} distributions also disappear when the samples were further cooked at higher temperature (data not shown).

Even though aging as previously mentioned has been found to increase meat's ability to retain inherent water (*1*, *10*), the structural changes and simultaneous water characteristics clearly do not promote the meat's ability to retain water upon cooking (Figure 1). The high cooking loss of aged samples reveals that the weakened protein structure during postmortem aging cannot tightly trap added water during cooking. Additionally, the increase in cooking loss in aged meat may be due to stronger aggregation of the proteins after aging. However, salting significantly reduced the difference in yield between nonaged and aged samples, which is consistent with the decreased difference in T_2 between nonaged and aged samples. This is the case because the decrease in T_2 generally reflects the shrinkage of myofibrils and loss of water, while the increase of T_2 indicates the swelling of meat protein and gain of water content (Figure 2). Furthermore, the decreased difference in yield between nonaged and aged samples with increasing salt concentration can be explained by the FT-IR data, as the good clustering according to aging was only well-observed for nonsalted and salted samples treated with 3% salt concentration in the score plots of PCA using the amide I region of FT-IR spectra as variables (Figure 5B). The cooking loss with increasing temperature can be ascribed to the increase in aggregated β-sheet structures and the decrease in native β-sheet and α-helical structures. The age-induced changes in protein secondary structure of cooked pork were the high content of α-helical structures, but salting weakened the difference of α-helical structures between nonaged and aged samples (Figure 6B).

The relationship between the changes in protein secondary structure and water distribution upon aging, salting, and cooking was also investigated using PLSR2. Cooking has the most dominating effect on observed changes in protein secondary structures and water distribution. Cooking causes a prominent increase in aggregated β-sheet structures and decrease in native β-sheet and α-helical structures, which contribute to the broadening of T_{21} distribution, decrease of relaxation times, and the loss of water upon cooking. The splitting of T_{21} distribution on cooking is supposed to be associated with the interaction of native and aggregated structures or transition state of protein denaturation. In uncooked samples, the dominating band of α-helices at 1653 cm^{-1} is linked to the T_2 relaxation times centered at 26−66 ms, reflecting myofibrillar water, and 232−285 ms, reflecting extra-myofibrillar water in raw meat. The increase of T_{21} relaxation times caused by salting may be related to the increase of β-sheet structures at 1682, 1639, 1628, and 1694 cm^{-1}. The increase of T_{22} relaxation times is probably associated with the increased aggregated β-sheet structures at 1628 and 1694 cm^{-1}. Finally, the relatively weak aging effect is not well-explained by the correlation-loading plot in both uncooked and cooked pork.

In conclusion, water distribution and changes in protein secondary structures in pork exposed to different aging times and subsequent salting and cooking were for the first time investigated using combined ^{1}H NMR relaxometry and FT-IR microspectroscopy. The increases in ^{1}H NMR T_2 relaxation times and the promoted water uptake caused by the interaction of aging time and salting are in addition to the well-known mechanisms also brought about by an increase in native β-sheet structure induced by salting and an increase of native α-helical structure induced by aging. The higher weight gain upon salting for aged pork is consistent with the increase of relaxation times for aged meat before cooking. The decrease of T_2 relaxation times, broadening of T_2 distribution, and loss of water upon cooking are attributed to the increase of aggregated β-sheet structure because of the thermal denaturation. The observed higher cooking loss in aged pork was counteracted through salting with increasing salt concentrations being most effective, which corresponds to the less evident effect of aging on protein secondary structural changes for samples treated with high salt concentrations.

ACKNOWLEDGMENT

We thank Marianne Rasmussen for technical assistance.

LITERATURE CITED

(1) Huff-Lonergan, E.; Longergan, S. M. Mechanisms of water-holding capacity of meat: The role of postmortem biochemical and structural changes. *Meat Sci.* **2005**, *71*, 194−204.

(2) Koohmaraie, M. Muscle proteinases and meat aging. *Meat Sci.* **1994**, *36*, 93−104.

(3) Zamora, F.; Debiton, E.; Lepetit, J.; Lebert, A.; Dransfield, E.; Ouali, A. Predicating variability of ageing and toughness in beef *m. longissimus lumborum et thoracis*. *Meat Sci.* **1996**, *43*, 321−333.

(4) Kristensen, L.; Purslow, P. P. The effect of ageing on the water-holding capacity of pork: role of cytoskeletal proteins. *Meat Sci.* **2001**, *58*, 17−23.

(5) Palka, K. The influence of post-mortem ageing and roasting on the microstructure, texture and collagen solubility of bovine *semitendinosus* muscle. *Meat Sci.* **2003**, *64*, 191−198.

(6) Straadt, I. K.; Rasmussen, M.; Andersen, H. J.; Bertram, H. C. Aging-induced changes in microstructure and water distribution in fresh and cooked pork in relation to water-holding capacity and cooking loss − A combined confocal laser scanning microscopy and low-field nuclear magnetic resonance relaxation study. *Meat Sci.* **2006**, accepted.

(7) Boakye, K.; Mittal, G. S. Changes in pH and water holding properties of *Longissimus dorsi* muscle during beef ageing. *Meat Sci.* **1993**, *34*, 335−349.

(8) Joo, S. T.; Kauffman, R. G.; van Laack, R. L. J. M.; Lee, S.; Kim, B. C. Variations in rate of water loss as related to different types of post-rigor porcine musculature during storage. *Food Chem. Toxicol.* **1999**, *5*, 865−868.

(9) Oreshkin, E. F.; Borissowa, M. A.; Permjakow, E. A.; Burstein, E. A. Konformationsveränderungen des Muskeleiweisses während der Reifung und ihre Beziehung zum Wasserbindungsvermögen von Schweinefleisch. *Fleischwirtschaft* **1989**, *69*, 627−630.

(10) Kristensen, L.; Purslow, P. P. The effect of ageing on the water-holding capacity of pork: role of cytoskeletal proteins. *Meat Sci.* **2001**, *58*, 17−23.

(11) Melody. J. L.; Lonergan, S. M.; Rowe, L. J.; Huiatt, T. W.; Mayes, M. S.; Huff-Lonergan, E. Early postmortem biochemical factors influence tenderness and water-holding capacity of three porcine muscles. *J. Anim. Sci.* **2004**, *82*, 1195−1205.
(12) Morison, E. H.; Mielche, M.; Purslow, P. P. Immunolocalisation of intermediate filament protein in porcine meat. Fibre type and muscle −specific variations during conditioning. *Meat Sci.* **1998**, *50*, 91−104.
(13) Lyon, C. E.; Dickens, J. A.; Lyon, B. G. Effects of electrical stimulation and postchill deboning time on texture and cook loss of broiler breasts processed under commercial conditions. *J. Appl. Poult. Res.* **2002**, 11217−222.
(14) Thygesen, G. L.; Løkke, M. M.; Micklander, E.; Engelsen, B. S. Vibrational microspectroscopy of food. Raman vs. FT-IR. *Trends Food Sci. Technol.* **2003**, *14*, 50−57.
(15) Reid, M. L.; O'Donnell, P. C.; Downey, G. Recent technological advances for the determination of food authenticity. *Trends Food Sci. Technol.* **2006**, *17*, 344−353.
(16) Van de Voort, F. R. Fourier transform infrared spectroscopy applied to food analysis. *Food Res. Int.* **1992**, *25*, 397−403.
(17) Duarte, I. F.; Barros, A.; Delgadillo, I.; Almeida, C.; Gil, A. M. Application of FTIR spectroscopy for the quantification of sugars in mango juice as a function of ripening. *J. Agric. Food Chem.* **2002**, *50*, 3104−3111.
(18) Tapp, H. S.; Defernez, M.; Kemsley, E. K. FTIR spectroscopy and multivariate analysis can distinguish the geographic origin of extra virgin olive oils. *J. Agric. Food Chem.* **2003**, *51*, 6110−6115.
(19) Ellis, D. I.; Broadhurst, D.; Goodacre, R. Rapid and quantitative detection of the microbial spoilage of beef by Fourier transform infrared spectroscopy and machine learning. *Anal. Chim. Acta* **2004**, *514*, 193−201.
(20) Mills, B. L.; van de Voort, F. R.; Kakuda, Y. The quantitative analysis of fat and protein in meat by transmission infrared analysis. *Meat Sci.* **1984**, *11*, 253−262.
(21) Fabian, H.; Mäntele, W. Infrared Spectroscopy of Proteins. In *Handbook of Vibrational Spectroscopy*; Chalmers, J. M., Griffiths, P. R., Eds.; John Wiley & Sons Ltd.: Chichester, 2002; pp 3399−3425.
(22) Dunlop, R. A.; Rodgers, K. J.; Dean, R. T. Recent developments in the intracellular degradation of oxidized proteins. *Free Radical Biol. Med.* **2002**, *33*, 894−906.
(23) Boskey, A. L.; Mendelsohn, R. Infrared spectroscopic characterization of mineralized tissues. *Vib. Spectrosc.* **2005**, *38*, 107−114.
(24) Kirschner, C.; Ofstad, R.; Skarpeid, H.-J.; Høst, V.; Kohler, A. Monitoring of denaturation processes in aged beef loin by Fourier transform infrared microspectroscopy. *J. Agric. Food Chem.* **2004**, *52*, 3920−3929.
(25) Bertram, H. C.; Kohler, A.; Böcker, U.; Ofstad, R.; Andersen, H. J. Heat-induced changes in myofibrillar protein structures and myowater of two pork qualities. A combined FT-IR spectroscopy and low-field NMR relaxometry study. *J. Agric. Food Chem.* **2006**, *54*, 1740−1747.
(26) Böcker, U.; Ofstad, R.; Bertram, H. C.; Egelandsdal, B.; Kohler, A. Salt-induced changes in pork myofibrillar tissue investigated by FT-IR microspectroscopy and light microscopy. *J. Agric. Food Chem.* **2006**, *54*; 6733−6740.
(27) Bertram, H. C.; Andersen, H. J. Applications of NMR in Meat Science. *Annu. Rep. NMR Spectrosc.* **2004**, *53*, 157−202.
(28) Micklander, E.; Peshlov, B.; Purslow, P. P.; Engelsen, S. B. NMR. cooking: The multiple states of water in meat during cooking. *Trends Food Sci. Technol.* **2002**, *13*, 341−346.
(29) Betram, H. C.; Karlsson, A. H.; Rasmussen, M.; Dønstrup, S.; Petersen, O. D.; Andersen, H. J. Origin of multi-exponential T2 relaxation in muscle myowater. *J. Agric. Food Chem.* **2001**, *49*, 3092−3100.
(30) Honikel, K. O. Reference methods for the assessment of physical characteristics of meat. *Meat Sci.* **1998**, *49*, 447−457.
(31) Andersen, R. H.; Andersen, H. J.; Bertram, H. C. Salting-induced water mobility and distribution within intra- and extra-myofibrillars of three pork qualities. *Int. J. Food Sci. Technol.* **2006**, in press.
(32) Bertram, H. C.; Engelsen, S. B.; Busk, H.; Karlsson, A. H.; Andersen, H. J. Water properties during cooking of pork studied by low-field NMR relaxation: effects of salting and the RN-gene. *Meat Sci.* **2004**, *66*, 437−446.
(33) Shaarani, S. M.; Nott, K. P.; Hall, L. D. Combination of moisture and structure changes for convection cooking of fresh chicken meat. *Meat Sci.* **2006**, *72*, 398−403.
(34) Brack, A.; Orgel, L. E. β structures of alternating polypeptides and their possible prebiotic significance. *Nature* **1975**, 256, 383−387.
(35) Ihara, S.; Ooi, T.; Takahashi, S. Effects of salts on the nonequivalent stability of the α-helices of isomeric block copolypeptides. *Biopolymers* **1982**, *21*, 131−145.
(36) Offer, G.; Trinick, J. On the mechanism of water holding in meat: the swelling and shrinking of myofibrils. *Meat Sci.* **1983**, *8*, 245−281.
(37) Wilding, P.; Hedges, N.; Lillford, P. J. Salt-induced swelling of meat: the effect of storage time, pH, ion-type and concentration. *Meat Sci.* **1986**, *18*, 53−75.
(38) Bertram, H. C.; Kristensen, M.; Andersen, H. J. Functionality of myofibrillar proteins as affected by pH, ionic strength and heat treatment − a low-field NMR study. *Meat Sci.* **2004**, *68*, 249−256.

Received for review June 6, 2006. Revised manuscript received August 21, 2006. Accepted August 24, 2006. Financial support by the Danish Meat and Bacon Council for funding the project "Process-induced structural changes in muscle proteins of importance for functional properties of meats" is gratefully acknowledged.

JF061576W